journal homepage: www.intl.elsevierhealth.com/journals/cmpb

A study on stability analysis of atrial repolarization variability using ARX model in sinus rhythm and atrial tachycardia ECGs

J. Sivaraman [a,*], G. Uma [b], P. Langley [c], M. Umapathy [b], S. Venkatesan [d], G. Palanikumar [b]

[a] Department of Biomedical Engineering, Vel Tech MultiTech, Chennai, India
[b] Department of Instrumentation and Control Engineering, National Institute of Technology, Tiruchirappalli, India
[c] School of Engineering, University of Hull, Hull, United Kingdom
[d] Department of Cardiology, Madras Medical College, Rajiv Gandhi Government General Hospital, Chennai, India

ARTICLE INFO

Article history:
Received 6 May 2016
Received in revised form
26 September 2016
Accepted 7 October 2016

Keywords:
Atrial repolarization dynamics
BIBO stability
Heart rate variability
Premature activation
PTa interval (PTaI)

ABSTRACT

Background: The interaction between the PTa and PP interval dynamics from the surface ECG is seldom explained. Mathematical modeling of these intervals is of interest in finding the relationship between the heart rate and repolarization variability.
Objective: The goal of this paper is to assess the bounded input bounded output (BIBO) stability in PTa interval (PTaI) dynamics using autoregressive exogenous (ARX) model and to investigate the reason for causing instability in the atrial repolarization process.
Methods: Twenty-five male subjects in normal sinus rhythm (NSR) and ten male subjects experiencing atrial tachycardia (AT) were included in this study. Five minute long, modified limb lead (MLL) ECGs were recorded with an EDAN SE-1010 PC ECG system. The number of minute ECGs with unstable segments (N_{us}) and the frequency of premature activation (PA) (i.e. atrial activation) were counted for each ECG recording and compared between AT and NSR subjects.
Results: The instability in PTaI dynamics was quantified by measuring the numbers of unstable segments in ECG data for each subject. The unstable segments in the PTaI dynamics were associated with the frequency of PA. The presence of PA is not the only factor causing the instability in PTaI dynamics in NSR subjects, and it is found that the cause of instability is mainly due to the heart rate variability (HRV).
Conclusion: The ARX model showed better prediction of PTa interval dynamics in both groups. The frequency of PA is significantly higher in AT patients than NSR subjects. A more complex model is needed to better identify and characterize healthy heart dynamics.

1. Introduction

Alternans of action potential duration (APD) create a repolarization dispersion which causes atrial fibrillation directly [1]. Initiation of cardiac arrhythmias is generally due to the unstable dynamics of APD at the cellular level which is responsible for the alternans in the repolarization phase [2,3]. In atrial ECG event, the Ta wave is represented as the repolarization phase and the PTa interval is the measure of total atrial ECG component which is the counterpart of QT interval of the ventricles.

* *Corresponding author.* Department of Biomedical Engineering, Vel Tech Multi Tech Engineering College. Chennai 600 062, India.
E-mail address: mountshiva@gmail.com (J. Sivaraman).
http://dx.doi.org/10.1016/j.cmpb.2016.10.005
0169-2607/

Abbreviations

AMI	acute myocardial infarction
APD	action potential duration
ARX	autoregressive exogenous
AT	atrial tachycardia
BIBO	bounded input bounded output
DI	diastolic interval
HRV	heart rate variability
MLL	modified limb lead
NSR	normal sinus rhythm
PA	premature activation
PTaI	PTa interval
PPI	PP interval
QTI	QT interval
TaPI	TaP interval

Abnormal atrial repolarization in ECG may be the key marker for different types of atrial arrthymia [4]. The clinical significance and alterations of the Ta wave and the P-Ta interval in atrial arrhythmias have been discussed by Childers [5] and Roukoz [6]. The atrial repolarization may be modified in its spatial orientation or in its duration by factors related to ischemic or necrotic phenomena and conditions that act upon the atria due to tachycardia, exercise and hyperthyroidism. These factors primarily affect repolarization, and the changes they produce are considered as primary alterations of atrial repolarization [7].

APD restitution refers to the cardiac action potential duration and its conduction velocity both depend on the previous diastolic interval (DI). The slope of APD restitution curve has been an indicator for the instability in the APD dynamics, and the cause of instability in the APD is mainly due to the occurrence of small perturbation in DI which results in a large (>1) APD restitution slope [8,9]. However, earlier studies have reported that the prediction of arrhythmia occurrence is not only due to APD restitution slope [10,11] but also been attributed to the presence of short-term memory [12,13].

Halamek et al. [14] investigated a transfer function based model for the adaptation of QT interval (QTI) with the alteration in heart rate. Chen et al. [15] used the QT-RR model to determine the QT dynamics stability and explored the contribution of premature activation (PA) and QTI instability to ventricular tachycardia onset. Chen et al. showed that the presence of PA in the ECG which is directly related with the unstable action potential dynamics could alter the normal QT variability. These unstable segments of the QTI dynamics could initiate arrhythmias like sustained ventricular tachycardia in acute myocardial infarction (AMI) patients. The instability in the QT dynamics could be a prognostic marker of the arrhythmia susceptibility for diseased human heart having prolonged QT interval, AMI and dilated cardiomyopathy [16]. Recently, Chen et al. [17] developed a novel methodology for assessing the BIBO instability criteria in QT interval dynamics. The authors introduced a short term linear ARX model for the prediction of the unstable segments in the ventricular repolarization characteristics and demonstrated the effect of the PA in QT interval dynamics stability by calculating the frequency of PA in ECG. Imam et al. [16] recently investigated in healthy subjects whether PA is the only reason for the instability criteria in the ventricular repolarization process using the same QT-RR model described by Chen et al. and found that the healthy heart showed high HRV and more asymmetry in comparison to the diseased heart. Recently, methods based on higher order spectra (HOS) statistics, principal component analysis, discrete wavelet transform and other computer aided diagnosis have been successfully demonstrated and utilized in the beat classification of atrial arrhythmias [18–24].

The electro physiological changes during atrial arrhythmia are well explained in several previous studies [25–27]. Atrial refractory period tends to become short as the atrial arrhythmia sustains longer, which is likely to have an influence on atrial repolarization phase. The properties of atrial repolarization might give rise to atrial arrhythmias in the same way as ventricular repolarization relates to ventricular arrhythmia [28].

In general, the electrocardiographic deflection of the atrial repolarization (Ta wave) is small in amplitude (μV) and generally it is obscured by the QRS complex in healthy subjects [4]. Hence during normal sinus rhythm (NSR), it is difficult to observe and record the Ta wave using the standard 12-lead ECG. To address the above limitations in recording the Ta wave morphology, the authors of this study proposed a novel modified limb lead (MLL) ECG recording system [29] for the study of atrial ECG components. In their subsequent studies, it was documented that a short sinus Ta wave segment was visible within the PR segment as a saucer-like depression [30], following the P wave and had an axis opposing the P wave approximately 180° in sinus rhythm subjects during normal PR prolongation. Also, they were able to determine the Ta peak amplitude within the PR segment in sinus rhythm subjects and further validated the MLL system for measuring the full Ta wave with different AV block patients [31,32]. The same authors studied the P and Ta wave morphology in healthy subjects using the P wave signal averaging method [33] and noted that the increase in the heart rate shortened the visible Ta wave segment and visible PTa interval in the healthy subjects. They also found that increase in age was a factor for the prolongation of the visible Ta wave and PTa interval.

Studies on the PTa interval dynamics using transfer function based model have not been reported so far, and analyzing the PTaI dynamics helps in understanding the mechanism of the onset of AT. In the present study, the main aim is to assess the BIBO stability in PTaI dynamics in normal sinus rhythm (NSR) and atrial tachycardia (AT) subjects from the ECGs recorded by the MLL system [29]. A linear ARX model [15] is used in this study to predict the PTaI dynamics. The functions are then transferred from time domain to their respective z-domain to predict the unstable segments. In addition, the ARX model complexity change is examined for the identification of the PTaI dynamics for NSR subjects in comparison to the AT patients. Also, a preliminary investigation is carried out whether the presence of PA beats is the only reason for the cause of unstable segments in PTaI of NSR and AT subjects.

2. Materials and methods

The methodology for identifying the instability in PTaI dynamics of both groups is carried out in two parts. First, the ARX model is represented as dependence of each PTaI on several

Table 1 – Basic statistics of the age of the subjects studied.

Age statistics
Sinus rhythm subjects 25 (29.4 ± 5.3) (20, 29, 40)
Atrial tachycardia patients 10 (54.5 ± 3.6) (50, 55, 59)
All subjects 35 (36.7 ± 12.6) (24, 32, 59)
Values are presented as n (mean ± S.D.) (minimum, median, and maximum).

prior PTaIs and PPIs. Second, the instability in PTaI dynamics of the ARX model is determined in the z-domain.

2.1. *Subjects*

This study was approved by the institutional ethics committee and all the subjects gave informed consent for participation in the study. The study cohort comprised two groups as described in Table 1. The patient group had 10 male patients with atrial tachycardia of mean age 54.5 ± 3.6 years (range 50 – 59 years). The second group had twenty-five male subjects of mean age 29.4 ± 5.3 years (range 20 – 40 years) in NSR. Both groups were recruited from the Rajiv Gandhi Government General Hospital, Chennai, India. Those in NSR were medically examined to exclude any form of cardiovascular disease. Smokers and patients with congestive heart failure, valvular disease and other cardiopulmonary diseases which may alter the ECG morphology were excluded from this study.

2.2. *Modified limb electrode placement*

The modified limb electrode placement [29] of the MLL system in which the bipolar limb electrodes are placed on the torso is shown in Fig. 1. The negative right arm electrode is placed on the subject's third right intercostal space, slightly to the left of the mid-clavicular line. The positive left arm electrode is placed in the 5th right intercostal space, slightly to the right of the mid-clavicular line, and the left leg electrode is placed in the 5th right intercostal space, on the mid-clavicular line. The right leg electrode is placed on the subject's right ankle. We use the standard notation such that lead I is the potential difference between right and left arm electrodes. The standard precordial electrode positions V_1–V_6 are unchanged.

2.3. *ECG data acquisition and analysis*

The MLL system [29,31] was used to record ECGs in the present study. Five minute long, MLL ECGs (in lead II configuration (Fig. 2)) were recorded at a standard ECG paper speed of 25 mm/s and 10 mm/mV in supine position in NSR and AT subjects using a digital electrocardiograph (EDAN SE-1010 PC ECG system, EDAN Instruments, Inc.,) operating at 1000 samples per second, with a frequency response of 0.05 Hz to 150 Hz. ECGs could be printed at variable gain from 2.5 mm/mV to 100 mm/mV and variable paper speed of 5 mm/s to 200 mm/s for the better delineation of ECGs. All the ECGs were recorded and transferred to a computer and stored for subsequent off-line processing. The digital data analysis of ECGs was performed using MATLAB (R 2012a) for Windows. Each 5 min ECG segments were then divided into 1 min long segments having 5 segments for each subject like the method presented by Chen et al. [15] and Imam et al. [16]. The analysis of HRV between the two groups was measured and analyzed separately for comparative purpose. The PTa interval, TaP interval (TaPI) and the total PP interval (PPI) were measured using the smart ECG measurement and interpretation programs of EDAN ECG machine in the present study, where PPI = PTaI + TaPI. Huikuri et al. [34] proposed a method for the count of premature activation from the RR time series for each 1 min ECG. The same method was used in this study for counting the PA from the PP time series. PA beat was detected each time when PP interval of a beat was shortened by at least 100 ms with respect to that of the preceding beat.

2.4. *Definitions*

In the MLL system ECG trace, the beginning of the P wave is denoted as P_{begin} and the peak of the P wave is denoted as P_{peak}. The end of the P wave was defined as the beginning of the Ta

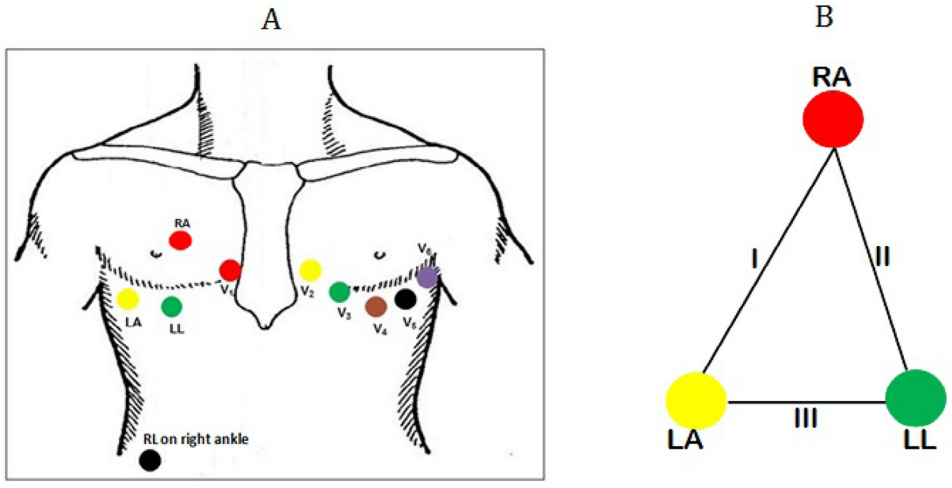

Fig. 1 – (a) Placement of limb electrodes on the torso. The precordial electrodes are unchanged. (b) Modified limb lead system.

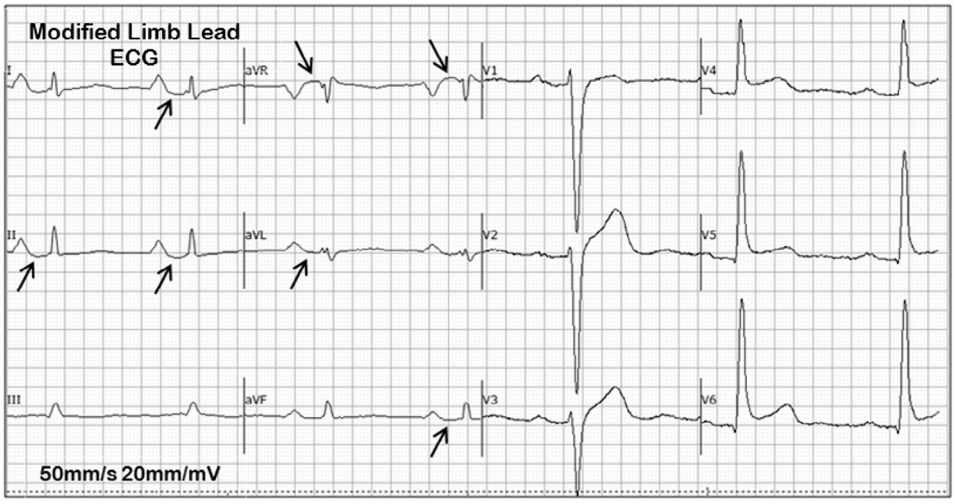

(a)

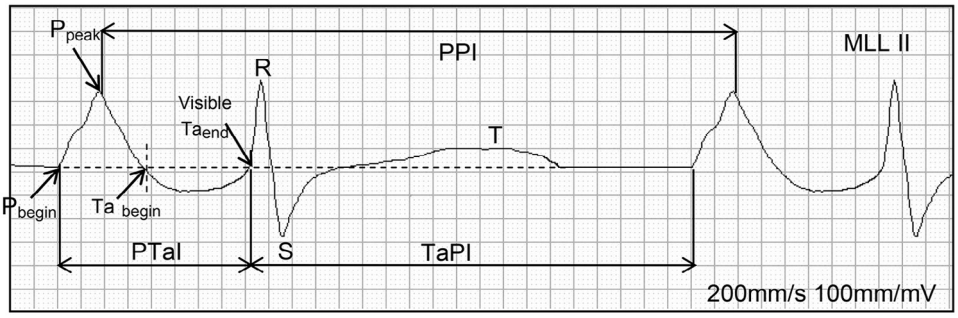

(b)

Fig. 2 – (a) Modified limb lead ECG of a sinus rhythm subject clearly shows the presence of atrial Ta wave as a depression in the PR segment of leads I, II and aVL with the corresponding reciprocal elevation in the lead aVR. (b) Modified limb lead ECG of a subject in sinus rhythm and the annotations of P_{begin}, Ta_{begin}, P_{peak}, visible Ta_{end}, TaPI and PPI. The ECG is replayed in 200 mm/s and 100 mm/mV for better delineation. One box has a width of 25 ms and a height of 0.05 mV.

wave (Ta_{begin}) at which the ECG trace crossed the isoelectric line [35]. The beginning of the Ta wave is denoted as Ta_{begin} and the visible end of Ta wave is denoted as visible Ta_{end}. The interval from the P_{begin} to the visible Ta_{end} was defined as the P-Ta interval [32]. The Ta_{begin} to the visible Ta_{end} was defined as the visible Ta duration [32]. All durations were annotated using the smart ECG measurement and interpretation programs of EDAN ECG machine to obtain PTaI, TaPI, and PPI as illustrated in Fig. 2.

2.5. *PTa-PP model formation*

The ARX [15] model for the PTaI dynamics is established using the system identification techniques. The dependence of the PTaI on the previous PTaIs and PPIs, an ARX model is developed for each 1 min ECG segment. The model equation is given by:

$$PTaI_n = \sum_{i=1}^{M} a_i^{1} \times PTaI_{n-i} + \sum_{i=1}^{N} b_i^{1} \times PPI_{n-i} \quad (1)$$

Where n is the beat number in 1 min ECG segment; PTaI and PPI are two discrete-time signals of the same length. $PTaI_n$, $PTaI_{n-i}$, and PPI_{n-i} are the values of the signal for beat n and $n-i$ respectively. The weight constants a_i and b_i for each preceding PTaI and PPI, respectively, contribute to $PTaI_n$. M and N represent the model order or the model parameters i.e., number of poles and zeros. The autoregressive term is $\sum_{i=1}^{M} a_i^{1} \times PTaI_{n-i}$, whereas the term $\sum_{i=1}^{N} b_i^{1} \times PPI_{n-i}$ represents the exogenous input. In Eq. (1), we used PPI instead of TaPI, because TaPI is affected by the preceding PTaI, and thus it is not an independent exogenous input. In this study, we have used M = N as described by Imam et al. which indicates that the memory effect [36] of heart rate and repolarization were considered in the model for prediction of PTaI dynamics. The parameter of each ARX model is evaluated using the System Identification Toolbox functions in MATLAB 7.14 (R2012a).

2.6. *Detection of stability in PTaI dynamics*

To detect and to determine the stability of the ARX model, the a_i and b_i coefficients are redefined and Eq. (1) can be rearranged as:

$$a_0^{1} PTaI_n - \sum_{i=1}^{M} a_i^{1} a_0^{1} \times PTaI_{n-i} = \sum_{i=1}^{N} b_i^{1} a_0^{1} \times PPI_{n-i} \quad (2)$$

Table 2 – Statistical summary of PPI, PTaI and TaPI of healthy subjects and AT patients.

Measurement		Sinus rhythm subjects	Atrial tachycardia patients	P value[a]
Atrial rate	bpm	76 ± 7.28	111 ± 4.87	
PPI	ms	786 ± 71.91	535 ± 21.86	<0.05
PTaI	ms	209 ± 12.23	163 ± 11.37	<0.05
TaPI	ms	577 ± 62.29	372 ± 12.11	<0.05

[a] Unpaired sample t-test.

$$a_0^{-1}PTaI_n + \sum_{i=1}^{M}\left(-a_i^{-1}a_0^{-1}\right)\times PTaI_{n-i} = \sum_{i=1}^{N} b_i^{-1}a_0^{-1}\times PPI_{n-i} \quad (3)$$

Assuming, $a_0^{-1} = a_0$; $-a_i^{-1}a_0^{-1} = a_i$; $b_i^{-1}a_0^{-1} = b_i$

$$a_0\times PTaI_n + \sum_{i=1}^{M} a_i\times PTaI_{n-i} = \sum_{i=1}^{N} b_i\times PPI_{n-i} \quad (4)$$

$$\sum_{i=0}^{M} a_i\times PTaI_{n-i} = \sum_{i=1}^{N} b_i\times PPI_{n-i} \quad (5)$$

Eq. (5) can be expanded as:

$$a_0PTaI_n + a_1PTaI_{n-1} + \ldots\ldots a_MPTaI_{n-M} = b_1PPI_{n-1} + b_2PPI_{n-2} + \ldots\ldots b_NPPI_{n-N} \quad (6)$$

Eq. (6) is the discrete-time expanded form of Eq (5). To study about stability of the PTa-PP ARX model, Eq. (6) is transformed into z-domain and represented in Eq. (7).

For each iteration of the model, the value of M was determined by increasing it from 1 for each step. The value of M was examined for each step whether the PTaI dynamics was accurately predicted in the minECG. The minimum number of poles required to detect the unstable segments in the PTaI is defined as M_{min} (low-order model), and the number of poles needed to achieve the predefined prediction capability is defined as M_{max} (high-order model). The value of M is increased from 1 sequentially up to the value when the model became unstable for the first time is calculated as M_{min}. M_{max} is the first value of M where the model achieved a predefined prediction value of the PTaI. In this study, the predefined accuracy of the mean square error between the predicted value and the measured PTaI value is smaller than 5 ms^2.

2.7. *BIBO stability analysis in PTaI dynamics*

The BIBO stability criterion was carried out for the ARX model of each ECG segments of the NSR subjects and AT patients. The ARX model was transformed from the time domain into the z-domain, where z is a complex number. The z transform [37] is then applied to Eq. (6), resulting in:

$$a_0PTaI(z) + a_1z^{-1}PTaI(z) + \ldots\ldots + a_Mz^{-M}PTaI(z) = b_1z^{-1}PPI(z) + b_2z^{-2}PPI(z) + \ldots\ldots + b_Nz^{-N}PPI(z) \quad (7)$$

The transfer function representation of Eq. (7) is given in Eq. (8).

$$H(z) = \frac{PTaI(z)}{PPI(z)} = \frac{b_1z^{-1} + b_2z^{-2} + \ldots\ldots + b_Nz^{-N}}{a_0 + a_1z^{-1} + \ldots\ldots + a_Mz^{-M}} \quad (8)$$

The factorized form of Eq. (8) to represent the poles (α_M) and zeros (β_N) of the model is given in Eq. (9) using which the pole-zero plot is illustrated.

The above equation can be represented in the factorized form as:

$$H(z) = \frac{PTaI(z)}{PPI(z)} = g\frac{(z-\beta_1)(z-\beta_2)\ldots\ldots(z-\beta_N)}{(z-\alpha_1)(z-\alpha_2)\ldots\ldots(z-\alpha_M)} \quad (9)$$

Eq. (9) is the transfer function H(z) of the ARX model in the z-domain. Where $\beta_1\ldots\beta_n$ are the zeros and $\alpha_1\ldots\ldots\alpha_n$ are the poles and g is the constant. Pole-zero cancellation occurs when they are equal. In this study, if the difference between a pole and a zero is smaller than 0.05, then a pole is practically canceled by a zero [17]. If any pole magnitude is greater than 1 (i.e. |pole| > 1) and when at least one pole was found to be outside the unit circle (i.e. |z| = 1) in the pole zero map, the model was considered unstable.

3. Results

Using the MLL ECG recordings from both groups, an ARX model was constructed for each minECG. The accuracy of the ARX model was studied by predicting the each value of PTaI in minECG. The atrial rate, duration of PPI, PTaI and TaPI of the groups are found to be statistically significant (P < 0.05) as shown in Table 2. Using the PPI of the minECG as input, the output of the model was computed for each subjects in this study. The ARX model output and the prediction error for an individual AT patient are shown in Fig. 3.

The ARX model was able to predict the measured PTaI dynamics accurately in one of the AT patients for $M_{max} = 26$ as shown in Fig. 3(a). While for $M_{min} = 9$, the model was not able to predict with the predefined mean square error of 5 ms^2 as shown in Fig. 3(b). The dependence of the prediction error on M for the same minECG is shown in Fig. 3(c). The same ARX model was also used to predict the measured PTaI dynamics in an individual NSR subject accurately for $M_{max} = 32$ and did not predict accurately for $M_{min} = 13$ as shown in Fig. 4(a) and 4(b) respectively. The dependence of the prediction error on M is shown in Fig. 4(c). The values of M_{min} and M_{max} for both groups are shown in Table 3, and the values between the model orders were found to be significantly different (P < 0.05). However, the

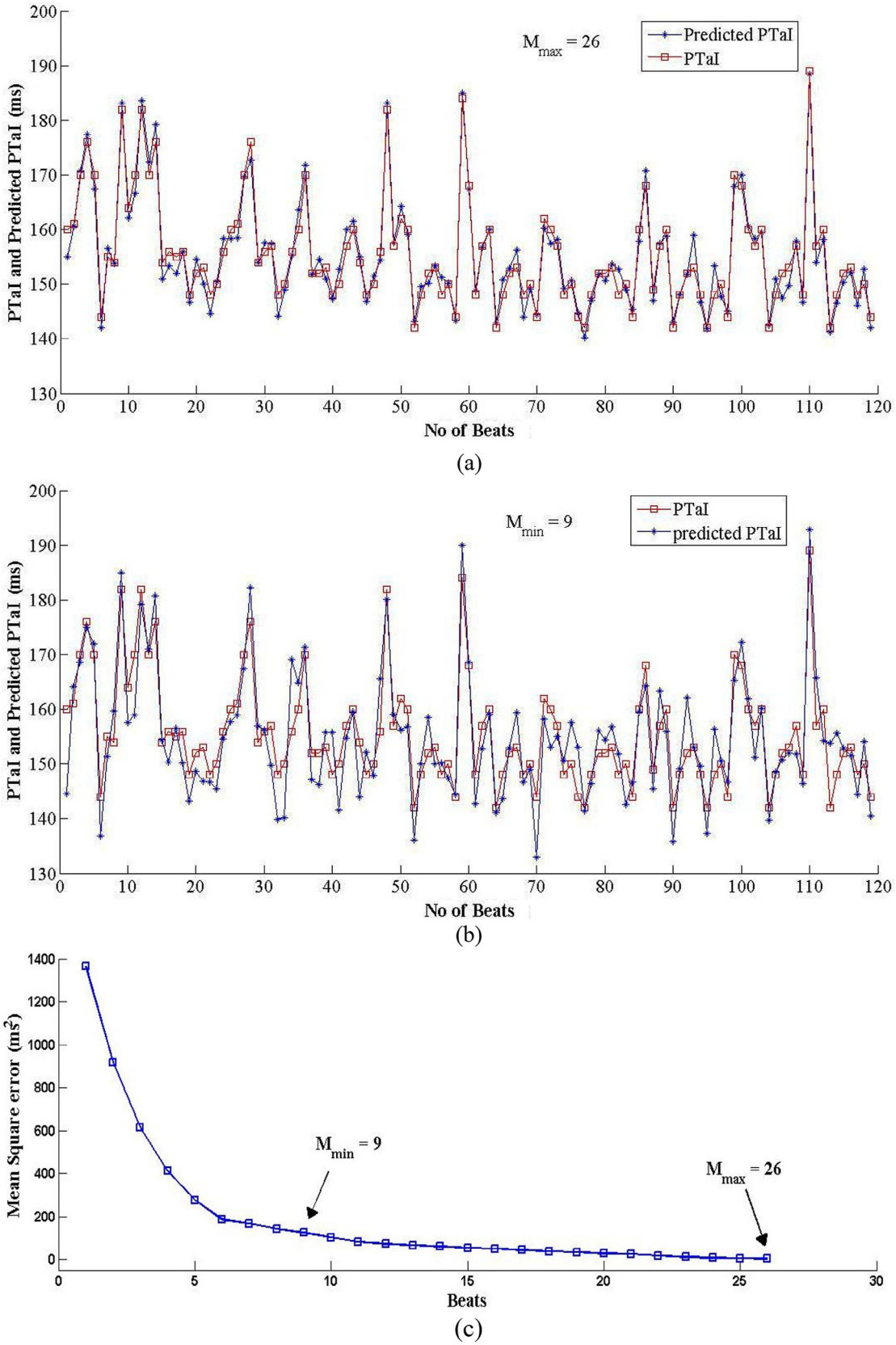

Fig. 3 – Predicted PTaI dynamics of a minECG for an individual AT patient by ARX model. (a) PTaI dynamics extracted from the minECG for M_{max} = 26. (b) PTaI dynamics extracted from the minECG for M_{min} = 9. (c) The dependence of the prediction error on M for the same minECG. M_{min} is the M at which unstable PTaI dynamics was first identified.

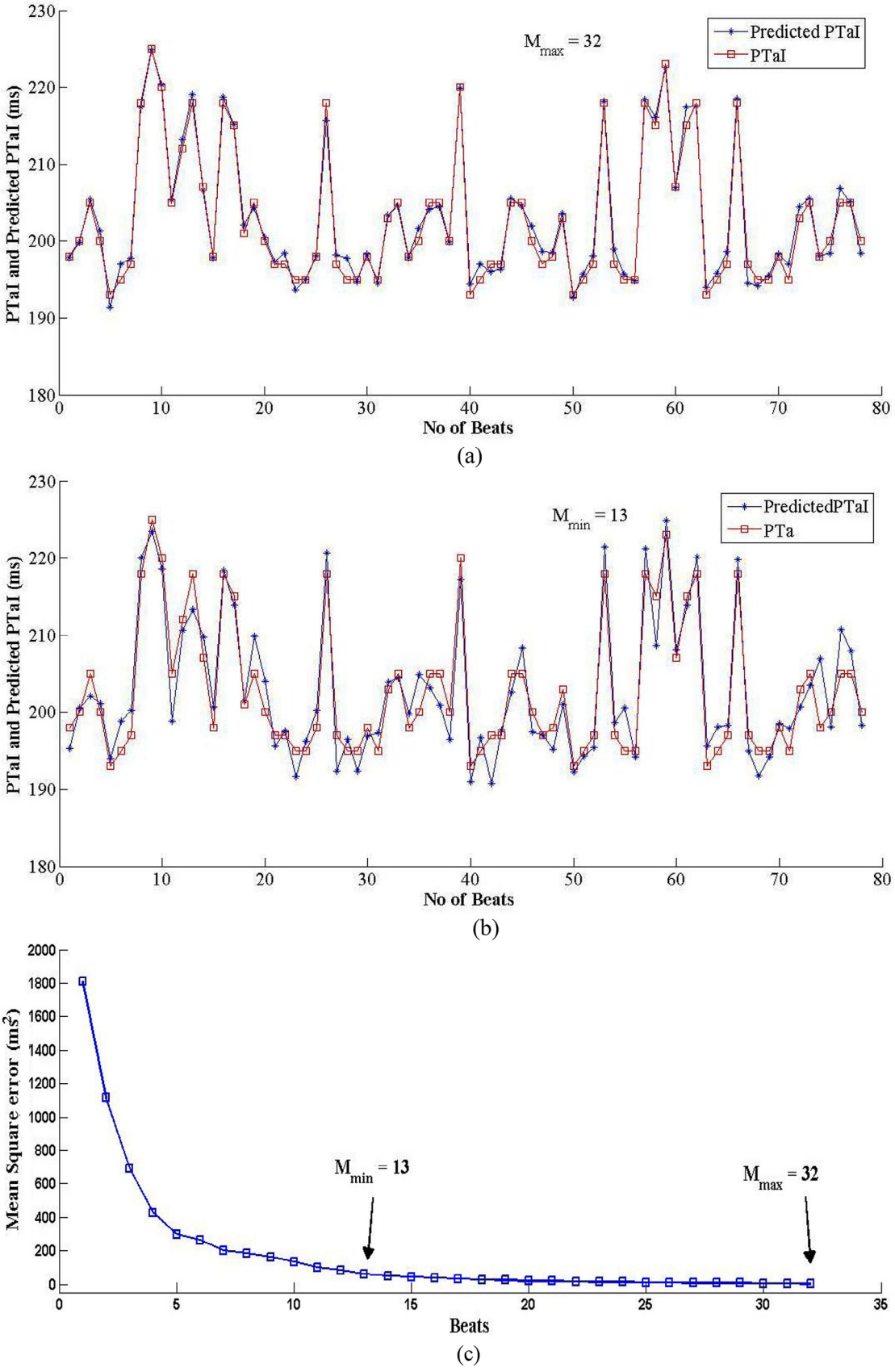

Fig. 4 – Predicted PTaI dynamics of a minECG for an individual NSR subject by ARX model. (a) PTaI dynamics extracted from the minECG for M_{max} = 32. (b) PTaI dynamics extracted from the minECG for M_{min} = 13. (c) The dependence of the prediction error on M for the same minECG. M_{min} is the M at which unstable PTaI dynamics was first identified.

Table 3 – Model order values of AT and NSR groups.

Feature	Atrial tachycardia (AT) subjects	Normal sinus rhythm (NSR) subjects	P value
Mmin	12.6 ± 3.05	28.6 ± 3.43	<0.05
Mmax	16.6 ± 2.59	33.2 ± 2.94	<0.05
N_{us}	3.2 ± 0.85	3.8 ± 0.94	>0.05

Values are presented as mean ± S.D.

difference between the numbers of unstable segment (N_{us}) for the two groups was found to be insignificant (P > 0.05).

The pole zero plots for the same minECG was obtained in the z domain. The stability analysis of the PTaI in the z domain for minECG of the same AT patient and NSR subject is shown in Fig. 5. The PTaI dynamics of this minECG for both groups are assessed as unstable, because the poles (marked with arrows) are outside the unit circle as seen in Fig. 5(a, b) for M = 9 and M = 26 for AT patient and M = 13 and M = 32 for NSR subject in Fig. 5(c, d). In the AT patient, the minimum number of poles required to detect the unstable segments is M_{min} = 9, and the maximum number of poles needed to achieve the predefined prediction capability is M_{max} = 26. From the pole zero plot of the AT patient, as the M value is increased from 9 to 26, new pole pairs are added as seen in Fig. 5(b). The locations of the two poles predicted by M_{min} in Fig. 5(a) remain the same as those in Fig. 5(b) (marked with arrows) even when the value of M is increased.

The same was observed for the NSR subject for M_{min} = 13 and M_{max} = 32, where the locations of the two poles predicted by M_{min} in Fig. 5(c) remain the same as those in Fig. 5(d) (marked with arrows) even when the value of M is increased. Analyses of the above result indicate that a higher value of M (M_{max}) is required for accurate prediction of PTaI dynamics, but the first occurrence of unstable segment is captured at a much

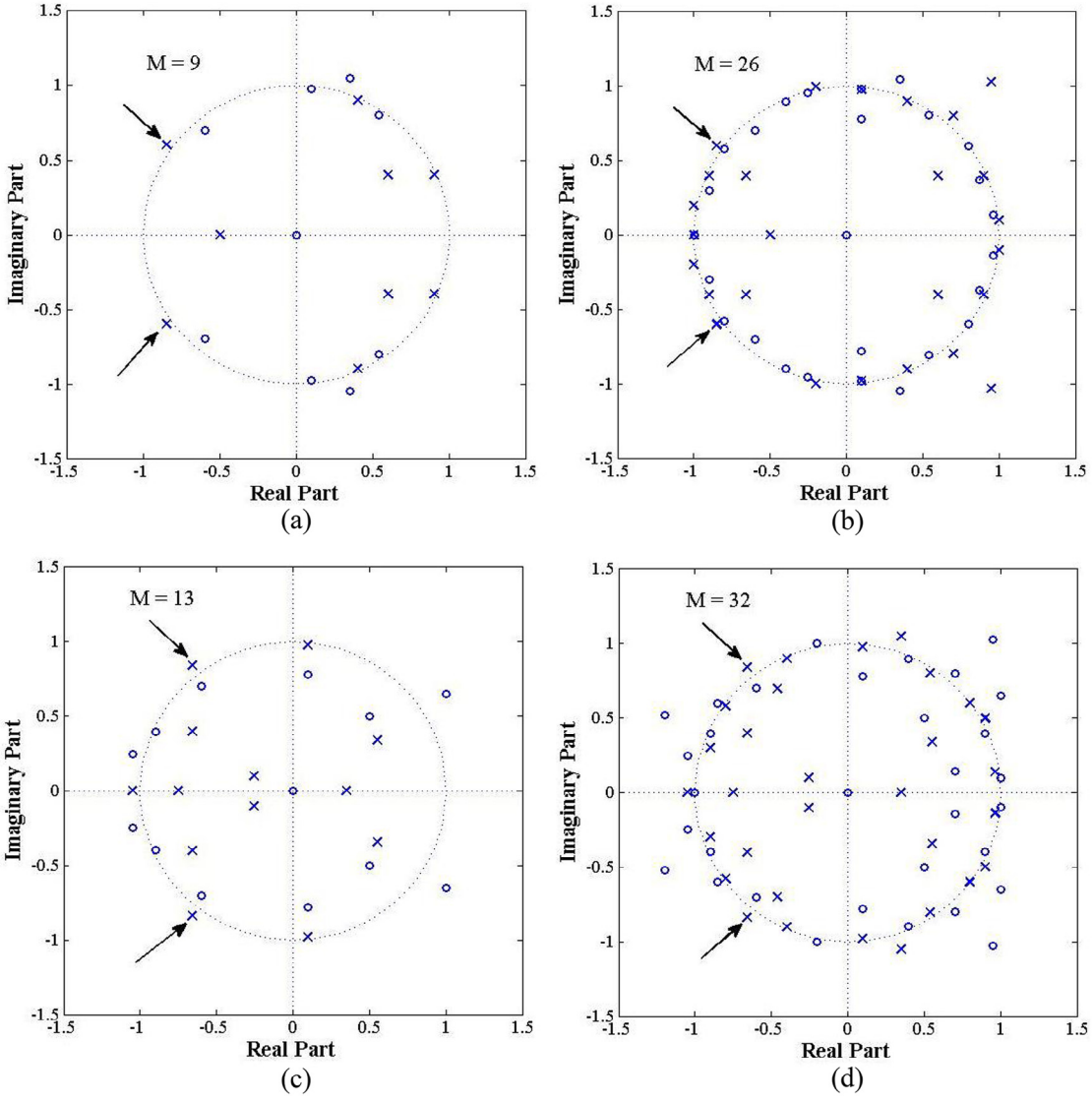

Fig. 5 – Pole-zero plots of minECG for an individual AT and NSR subject using ARX model. (a, b) Pole-zero plot in AT patient for M_{min} = 9 and M_{max} = 26. (c, d) Pole-zero plot in NSR subject for M_{min} = 13 and M_{max} = 32.

Table 4 – Number of stable and unstable segments in AT and NSR groups.

Group	Stable segments	Unstable segments	Total segments
Atrial tachycardia (AT) patients	14	36	50
Normal sinus rhythm (NSR) subjects	47	78	125

smaller M (M_{min}) in both groups. The distribution of stable and unstable segments in the PTaI of both groups is shown in Table 4.

4. Discussions

4.1. *BIBO stability analysis in PTa-PP model*

The autoregressive model used by Chen et al. [17] was aimed for the stability analysis of ventricular repolarization process with RR interval used as the exogenous input in the model. In the study done by Chen et al., the authors did not consider any additional noise term in their model that may induce instability in the QTI dynamics. In the present study, the same methodology was used to predict the BIBO stability in the atrial repolarization process with PP interval as the exogenous input in the PTa-PP model. The derived ARX model was able to predict the PTaI dynamics in NSR and AT subjects, and the model was validated with the measured PTaI and PPI, and the mean square error was found to be within the tolerance (5 ms^2). Using this methodology, we were able to demonstrate that the PTaI dynamics becomes unstable for every PA beats.

4.2. *Effect of premature activation in PTaI dynamics*

Imam et al. [16] used the same model for studying the QTI dynamics in healthy subjects and AT patients. The main aim of their study is to investigate whether the PA is the only reason for instability in the QTI dynamics and found that the presence of PA might not be the only factor for instability in QTI dynamics as concluded by Chen et al. They reported that the heart rate variability on the QTI dynamics in healthy subjects is more complex compared to the AT patients and also noted that the presence and absence of PAs is not the only cause for the instability and stability in the repolarization process. Imam et al. suggested that a nonlinear model for stability analysis could enable better explanation of healthy heart dynamics as healthy heart shows high HRV and more asymmetry in comparison to diseased heart [38].

The model complexity changes is examined for the identification of the PTaI dynamics for NSR subjects in comparison to the AT patients, and it is found that the ARX model prediction capability is significant in detecting the PTaI dynamics. From the results of this study it is obvious that the absence of PAs might not be the only reason for stability in PTaI dynamics, since many of the 1 min ECG segments became unstable for NSR subjects which were free from PA beats. Similarly, the presence of PAs may not be the reason for the ECG segments to become unstable in NSR subjects since the effect of HRV would have caused unstable segments in the ECG which is in agreement with the previous study as described by Imam et al. [16] in healthy subjects. The present investigation also reveals that the unstable PTaI dynamics were correlated with the frequency of PAs which is in agreement with the previous study done by Chen et al.

4.3. *Effect of heart rate variability on the PTaI dynamics*

In the present work, the ARX model was used to study the effect of HRV on PP interval and PTa interval in NSR subjects and AT patients. Since the PTa interval affects the subsequent TaP interval, we studied the HRV based on analyzing the PP interval which includes both the TaP and PTa interval within it. The time domain analysis and comparison of HRV between the two groups is shown in Table 5. Several previous studies have established that QTI is not only affected by heart rate variability, and other factors like respiration, temperature, gender, age, genetic profile and autonomic nervous system have an effect on the QTI [39,40]. Similar to the QTI variability, Debbas et al. [35] studied the effects of the sinus rate, pacing and drugs on the Ta wave in heart block patients and noted the variations in the PTaI dynamics.

Recently, Sivaraman et al. [33] studied the P and Ta wave morphology in healthy subjects and noted that the increase in age prolonged the P and Ta wave duration and increase in the heart rate shortened the observable P-Ta interval in the healthy subjects. From the results of this study, it is evident that the PAs are not the only reason in causing the unstable segments in NSR subjects likewise in the AT patients. Seen in the light of these findings, it is obvious that the cause of unstable segments of PTaI in NSR subjects is mainly due to the HRV and also due to the other intrinsic factors as described in Refs. [39,40]. Acharya et al. documented that healthy heart showed high HRV and more asymmetry compared with the diseased heart. Perhaps this could be the reason why the ARX

Table 5 – Comparison of HRV between the NSR and AT groups.

Measurement		Normal sinus rhythm subjects	Atrial tachycardia patients	P value[a]
Atrial rate	bpm	76 ± 7.28	116 ± 4.87	<0.05
Average PPI (AVNN)	ms	786 ± 71.91	535 ± 21.86	<0.05
Max PPI	ms	899 ± 88.92	584 ± 35.92	<0.05
Min PPI	ms	676 ± 73.69	496 ± 14.31	<0.05
SDNN	ms	51 ± 23.21	17 ± 5.89	<0.05
RMSSD	ms	45 ± 16.41	12 ± 3.68	<0.05

[a] Unpaired sample t-test.

model in this study actually needed high-order model (M_{max}) to predict the PTaI dynamics accurately in NSR subject than the AT patients. Since the healthy heart involves intricate dynamics, more complex model is required to understand such effect on PTaI dynamics.

From this preliminary investigation, it is found that the presence of PA might not be the only factor for causing the instability in PTaI in NSR subjects. The instability in NSR subjects is mainly due to high HRV within the subject which required high-order model to detect the instability. Further analysis to find the prediction capability of the ARX model was achieved by increasing the model order in predicting the PTaI dynamics in both groups.

5. Conclusion

In this study, the ARX methodology was proposed to assess the atrial repolarization dynamics in clinical ECG interpretation. The derived ARX model predicted the PTaI dynamics in NSR and AT subjects, and the model was validated with the measured PTaI and PPI. In the present study, it is found that the presence of unstable segments in the AT patients was generally due to premature activation. But the results of this study showed that similar number of unstable segments was seen for both the AT and NSR subjects. The unstable segments in NSR subjects are mainly due to the HRV within the subjects. Obviously, future larger studies using more complex model are needed to shed light on the prediction of the PTaI dynamics and the presence of PAs in healthy heart dynamics. Further studies are warranted to analyze the effects of anti-arrhythmic drugs on the stability of PP-PTa interval.

5.1. *Clinical implications*

Atrial repolarization abnormalities and APD dynamics are the major electrophysiological substrate for atrial arrhythmia. The PTa interval represents the atrial repolarization phase, and a premature atrial activity falling on this period can trigger a sustained atrial arrhythmia or even an atrial fibrillation. The risk of atrial fibrillation can be manifold higher if the PTa interval is prolonged for any reason like drug effect, ischemia, or structural atria disease. Analyzing the alternans and unstable APD dynamics using a mathematical model is of interest in clinical monitoring and medical decision making in recent years. The results of this study demonstrates that the ARX model representing the ECG signals can be applied in finding the onset and development of PTaI instability due to premature activation and heart rate variability in diseased and healthy hearts. Analyzing the PTaI and PPI stability helps in understanding the mechanisms of the onset of arrhythmia. The present study can be extended to study the alternans of Ta wave segment and PTaI dynamics in different AV block patients where the full Ta wave can be accessed due to AV conduction block.

5.2. *Study limitations*

The ARX model is now well established for the study of QTI dynamics and the extension of the method to enable the study of PTaI dynamics is not likely to affect the validity of the model. The later part of the Ta wave is not observed in sinus rhythm subjects and AT patients, and this limitation restricted us to study the later part of the atrial repolarization dynamics. Although the later part of Ta wave is seen, it is unlikely that enough information can be obtained from the analysis of the later Ta wave segment to differentiate the instability of the PTaI dynamics from the visible segment. The ARX model used in this study is not capable of decoupling the artifacts in ECG signals from the system dynamics. This study requires a long duration recording of ECGs which is greater than the standard clinical measurement duration (>10 seconds).

Conflict of interest

None of the authors have any conflict of interest to declare.

Acknowledgments

One of the authors would like to thank the fund from the DST-FIST, Government of India, vide Ref.: SR/FST/College-189/2013, Dated: 6th August 2014. This research work was carried out in Madras Medical College, Rajiv Gandhi Government General Hospital, Chennai.

REFERENCES

[1] S.M. Narayan, M.R. Franz, P. Clopton, E.J. Pruvot, D.E. Krummen, Repolarization alternans reveals vulnerability to human atrial fibrillation, Circulation 123 (2011) 2922–2930.
[2] M.L. Koller, M.L. Riccio, R.F. Gilmour, Dynamic restitution of action potential duration during electrical alternans and ventricular fibrillation, Am. J. Physiol. 275 (1998) H1635–H1642.
[3] Z. Qu, A. Garfinkel, P.S. Chen, J.N. Weiss, Mechanisms of discordant alternans and induction of reentry in simulated cardiac tissue, Circulation 102 (2000) 1664–1670.
[4] D.I. Abramson, N.M. Fenichel, C. Shookhoff, A study of electrical activity in the auricles, Am. Heart J. 15 (1938) 471–481.
[5] R. Childers, Atrial repolarization: its impact on electrocardiography, J. Electrocardiol. 44 (2011) 635–640.
[6] R. Henri, W. Kyuhyun, Response to letter to the editor, Ann. Noninvasive Electrocardiol. 16 (2011) 416–417.
[7] T. Joao, A.J. Victor, D.O. Martin, Atrial repolarization—its importance in clinical electrocardiography, Circulation 22 (1960) 635–644.
[8] J.B. Nolasco, R.W. Dahlen, A graphic method for the study of alternation in cardiac action potentials, J. Appl. Physiol. 25 (1968) 191–196.
[9] E.C. Ifeachor, B.W. Jervis, Digital Signal Processing, second ed., Prentice-Hall, Englewood Cliffs, NJ, 2002.
[10] I. Banville, R.A. Gray, Effect of action potential duration and conduction velocity restitution and their spatial dispersion on alternans and the stability of arrhythmias, J. Cardiovasc. Electrophysiol. 13 (2002) 1141–1149.
[11] E.M. Cherry, F.H. Fenton, Suppression of alternans and conduction blocks despite steep APD restitution: electrotonic, memory, and conduction velocity restitution

effects, Am. J. Physiol. Heart Circ. Physiol. 286 (2004) H2332–H2341.
[12] N.F. Otani, R.F. Gilmour, Memory models for the electrical properties of local cardiac systems, J. Theor. Biol. 187 (1997) 409–436.
[13] R.F. Gilmour, N.F. Otani, M.A. Watanabe, Memory and complex dynamics in cardiac Purkinje fibers, Am. J. Physiol. 272 (1997) H1826–H1832.
[14] J. Halamek, P. Jurak, M. Villa, M. Novak, V. Vondra, M. Soucek, et al., Dynamic QT/RR coupling in patients with pacemakers, in: Proc. 29th IEEE Int. Conf. on Eng. Med. Biol. Soc. Lyon, France, 2007, pp. 919–922.
[15] X. Chen, Y. Hu, B.J. Fetics, R.D. Berger, N.A. Trayanova, Unstable QT interval dynamics precedes ventricular tachycardia onset in patients with acute myocardial infarction: a novel approach to detect instability in QT interval dynamics from clinical ECG, Circ. Arrhythm. Electrophysiol. 4 (2011) 858–866.
[16] M.H. Imam, C.K. Karmakar, A.H. Khandoker, M. Palaniswami, Effect of premature activation in analyzing QT dynamics instability using QT-RR model for ventricular fibrillation and healthy subjects, in: Proc. 35th IEEE Int. Conf. Eng. Med. Biol. Soc. Osaka, Japan, 2013, pp. 3–7.
[17] X. Chen, N.A. Trayanova, A novel methodology for assessing the bounded-input bounded-output instability in QT interval dynamics: application to clinical ECG with ventricular tachycardia, IEEE Trans. Biomed. Eng. 59 (2012) 2111–2117.
[18] R.J. Martis, U.R. Acharya, K.M. Mandana, A.K. Ray, C. Chakraborty, Application of principal component analysis to ECG signals for automated diagnosis of cardiac health, Expert Syst. Appl. 39 (2012) 11792–11800.
[19] R.J. Martis, U.R. Acharya, K.M. Mandana, A.K. Ray, C. Chakraborty, Cardiac decision making using higher order spectra, Biomed. Signal Proces. 8 (2013) 193–203.
[20] R.J. Martis, U.R. Acharya, L.C. Min, ECG beat classification using PCA, LDA, ICA and discrete wavelet transform, Biomed. Signal Proces. 8 (2013) 437–448.
[21] R.J. Martis, U.R. Acharya, H. Prasad, C.K. Chua, C.M. Lim, J.S. Suri, Application of higher order statistics for atrial arrhythmia classification, Biomed. Signal Proces. 8 (2013) 888–900.
[22] R.J. Martis, U.R. Acharya, C.M. Lim, J.S. Suri, Characterization of ECG beats from cardiac arrhythmia using discrete cosine transform in PCA framework, Knowl.-Based Syst. 45 (2013) 76–82.
[23] R.J. Martis, U.R. Acharya, H. Adeli, Current methods in electrocardiogram characterization, Comput. Biol. Med. 48 (2014) 133–149.
[24] R.J. Martis, U.R. Acharya, H. Adeli, H. Prasad, J.H. Tan, K.C. Chua, et al., Computer aided diagnosis of atrial arrhythmia using dimensionality reduction methods on transform domain representation, Biomed. Signal Proces. 13 (2014) 295–305.
[25] M.C. Wijffels, C.J. Kirchhof, R. Dorland, M.A. Allessie, Atrial fibrillation begets atrial fibrillation. A study in awake chronically instrumented goats, Circulation 92 (1995) 1954–1968.
[26] C.A. Morillo, G.J. Klein, D.L. Jones, C.M. Guiraudon, Chronic rapid atrial pacing. Structural, functional, and electrophysiological characteristics of a new model of sustained atrial fibrillation, Circulation 91 (1995) 1588–1595.
[27] M. Allessie, J. Ausma, U. Schotten, Electrical, contractile and structural remodeling during atrial fibrillation, Cardiovasc. Res. 54 (2002) 230–246.
[28] J.A. Abildskov, M.J. Burgess, P.M. Urie, R.L. Lux, R.F. Wyatt, The unidentified information content of the electrocardiogram, Circ. Res. 40 (1977) 3–7.
[29] J. Sivaraman, G. Uma, S. Venkatesan, M. Umapathy, V.E. Dhandapani, Normal limits of ECG measurements related to atrial activity using a modified limb lead system, Anatol. J. Cardiol. 15 (2015) 2–6.
[30] J. Sivaraman, G. Uma, M. Umapathy. A modified chest leads for minimization of ventricular activity in electrocardiograms. In: Proceedings of the International Conference on Biomedical Engineering; 2002 Feb 27–28, Penang, Malaysia; 2002 pp. 79–82.
[31] J. Sivaraman, G. Uma, S. Venkatesan, M. Umapathy, V.E. Dhandapani, A novel approach to determine atrial repolarization in electrocardiograms, J. Electrocardiol. 46 (2013) e1.
[32] J. Sivaraman, G. Uma, S. Venkatesan, M. Umapathy, M.S. Ravi, Unmasking of atrial repolarization waves using a simple modified limb lead system, Anatol. J. Cardiol. 15 (2015) 605–610.
[33] J. Sivaraman, G. Uma, S. Venkatesan, M. Umapathy, N. Keshav Kumar, A study on atrial Ta wave morphology in healthy subjects: an approach using P wave signal-averaging method, J. Med. Imaging Health Inf. 4 (2014) 675–680.
[34] H.V. Huikuri, J.O. Valkama, K.E. Airaksinen, T. Seppanen, K.M. Kessler, J.T. Takkunen, et al., Frequency domain measures of heart rate variability before the onset of nonsustained and sustained ventricular tachycardia in patients with coronary artery disease, Circulation 87 (1993) 1220–1228.
[35] N.M. Debbas, S.H. Jackson, D. de Jonghe, A. Robert, A.J. Camm, Human atrial repolarization: effects of sinus rate, pacing and drugs on the surface electrocardiogram, J. Am. Coll. Cardiol. 33 (1999) 358–365.
[36] J. Huang, X. Zhou, W.M. Smith, R.E. Ideker, Restitution properties during ventricular fibrillation in the in situ swine heart, Circulation 110 (2004) 3161–3167.
[37] L. Ljung, System Identification Theory for the User, second ed., Prentice-Hall PTR, Upper Saddle River, NJ, 1999.
[38] U.R. Acharya, K.P. Joseph, N. Kannathal, C.M. Lim, J.S. Suri, Heart rate variability: a review, Med. Biol. Eng. Comput. 44 (2006) 1031–1051.
[39] A. Porta, E. Tobaldini, T. Gnecchi-Ruscone, N. Montano, RT variability unrelated to heart period and respiration progressively increases during graded head-up tilt, Am. J. Physiol. Heart Circ. Physiol. 298 (2010) H1406–H1414.
[40] J.P. Couderc, Measurement and regulation of cardiac ventricular repolarization: from the QT interval to repolarization morphology, Phil. Trans. R. Soc. A 367 (2009) 1283–1299.